The EMBO Journal (2013) 32, 1265–1279
www.embojournal.org

TRANSPARENT PROCESS

THE EMBO JOURNAL

Mitochondria-type GPAT is required for mitochondrial fusion

Yohsuke Ohba[1], Takeshi Sakuragi[1,6], Eriko Kage-Nakadai[2,3], Naoko H Tomioka[1], Nozomu Kono[1,3], Rieko Imae[1,2,3], Asuka Inoue[4], Junken Aoki[4], Naotada Ishihara[5], Takao Inoue[1,3,7], Shohei Mitani[2,3] and Hiroyuki Arai[1,3,*]

[1]Department of Health Chemistry, Graduate School of Pharmaceutical Sciences, University of Tokyo, Tokyo, Japan, [2]Department of Physiology, Tokyo Women's Medical University School of Medicine, Tokyo, Japan, [3]CREST, Japan Science and Technology Agency (JST), Tokyo, Japan, [4]Laboratory of Molecular and Cellular Biochemistry, Graduate School of Pharmaceutical Sciences, Tohoku University, Sendai, Japan and [5]Department of Protein Biochemistry, Institute of Life Science, Kurume University, Kurume, Japan

Glycerol-3-phosphate acyltransferase (GPAT) is involved in the first step in glycerolipid synthesis and is localized in both the endoplasmic reticulum (ER) and mitochondria. To clarify the functional differences between ER-GPAT and mitochondrial (Mt)-GPAT, we generated both GPAT mutants in *C. elegans* and demonstrated that Mt-GPAT is essential for mitochondrial fusion. Mutation of Mt-GPAT caused excessive mitochondrial fragmentation. The defect was rescued by injection of lysophosphatidic acid (LPA), a direct product of GPAT, and by inhibition of LPA acyltransferase, both of which lead to accumulation of LPA in the cells. Mitochondrial fragmentation in Mt-GPAT mutants was also rescued by inhibition of mitochondrial fission protein DRP-1 and by overexpression of mitochondrial fusion protein FZO-1/mitofusin, suggesting that the fusion/fission balance is affected by Mt-GPAT depletion. Mitochondrial fragmentation was also observed in Mt-GPAT-depleted HeLa cells. A mitochondrial fusion assay using HeLa cells revealed that Mt-GPAT depletion impaired mitochondrial fusion process. We postulate from these results that LPA produced by Mt-GPAT functions not only as a precursor for glycerolipid synthesis but also as an essential factor of mitochondrial fusion.

The EMBO Journal (2013) **32,** 1265–1279. doi:10.1038/emboj.2013.77; Published online 9 April 2013
Subject Categories: membranes & transport; cellular metabolism
Keywords: *C. elegans*; fusion; glycerol-3-phosphate acyltransferase; lysophosphatidic acid; mitochondria

*Corresponding author. Graduate School of Pharmaceutical Sciences, University of Tokyo, 7-3-1, Hongo, Bunkyo-ku, Tokyo 113-0033, Japan. Tel.: +81 3 5841 4720; Fax: +81 3 3818 3173;
E-mail: harai@mol.f.u-tokyo.ac.jp
[6]These authors contributed to equally to this work
[7]Present address: Division of Cellular and Gene Therapy Products, National Institute of Health Sciences, Tokyo 158-8501, Japan

Received: 16 October 2012; accepted: 12 March 2013; published online: 9 April 2013

Introduction

Glycerolipids, which include phospholipids and triacylglycerol, are ubiquitous and important biological components. Phospholipids are the major constituents of biological membranes, playing important roles in multiple cellular processes including maintenance of the cellular permeability barrier, regulation of the activities of proteins associated with the membrane, and regulation of intracellular signalling by serving as precursors of signalling molecules (Dowhan, 1997). Triacylglycerol is a major storage form of energy, as well as being a major component of secreted lipoproteins. The biosynthetic pathways for these glycerolipids have been well established (Kent, 1995; Dowhan, 1997). The initial and rate-limiting step of glycerolipid synthesis is the acylation of glycerol-3-phosphate (G3P) with long-chain fatty acyl-CoA to form lysophosphatidic acid (LPA). This reaction is catalysed by glycerol-3-phosphate acyltransferase (GPAT) (Coleman *et al*, 2000; Wendel *et al*, 2009). LPA is further acylated by LPA acyltransferase (LPAAT) located at the ER to form phosphatidic acid (PA), a common precursor for phospholipid and triacylglycerol synthesis (Coleman and Lee, 2004; Takeuchi and Reue, 2009). To date, four mammalian GPATs have been identified and classified into two groups based on sequence homology and subcellular localization (Figure 1A; Gimeno and Cao, 2008; Wendel *et al*, 2009). GPAT1 and GPAT2 are mitochondrial GPATs that are localized to the mitochondrial outer membrane, and GPAT3 and GPAT4 are microsomal GPATs that are localized to the endoplasmic reticulum (ER) membrane (Gimeno and Cao, 2008; Wendel *et al*, 2009). All four of these GPATs are members of the AGPAT (1-acyl-sn-glycerol-3-phosphate acyltransferase) family that contain four conserved AGPAT motifs (Neuwald, 1997). Mitochondrial GPAT1 knockout (GPAT1$^{-/-}$) mice (Hammond *et al*, 2002) and microsomal GPAT4 knockout (GPAT4$^{-/-}$) mice (Vergnes *et al*, 2006) exhibited reduced triacylglycerol content in the liver. GPAT4$^{-/-}$ mice also showed large reductions in the triacylglycerol contents in adipose tissue, subdermal fat, and milk (Beigneux *et al*, 2006; Vergnes *et al*, 2006), while GPAT1$^{-/-}$ mice showed increased hepatic fatty acid oxidation and altered insulin resistance when fed a high fat diet (Hammond *et al*, 2005; Neschen *et al*, 2005; Yazdi *et al*, 2008). Significant GPAT activity remains in the mitochondrial and microsomal fractions in the GPAT1$^{-/-}$ and GPAT4$^{-/-}$ mice, respectively, suggesting that GPAT2 and GPAT3 compensate for the functions of mitochondrial and microsomal GPATs in mice (Lewin *et al*, 2004; Chen *et al*, 2008; Nagle *et al*, 2008). However, the effects of knocking out both mitochondrial GPATs (GPAT1 and GPAT2) or both microsomal GPATs (GPAT3 and GPAT4) have not yet been examined.

Most of the enzymes of glycerolipid biosynthesis reside in the ER membrane, but GPATs are also located on the mitochondrial outer membrane, which raises a question: Why is LPA synthesized in both mitochondria and ER? To answer this

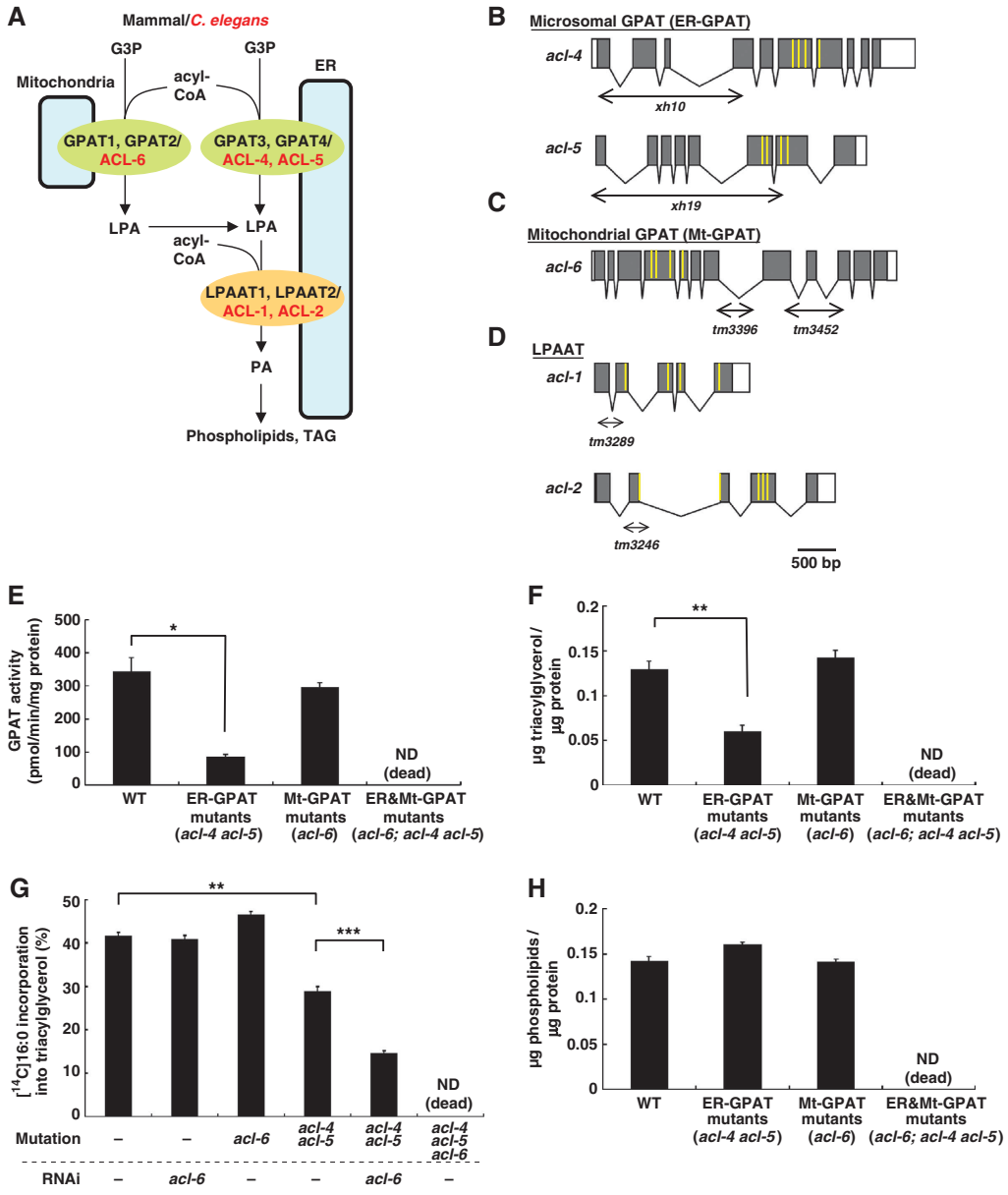

Figure 1 *C. elegans* GPATs, *acl-4, acl-5,* and *acl-6,* contribute to triacylglycerol synthesis. (**A**) In mammals and *C. elegans*, glycerol-3-phosphate acyltransferases (GPATs) are located on both the outer mitochondrial membrane (mitochondrial GPAT) and endoplasmic reticulum (ER) (microsomal GPAT) to produce lysophosphatidic acid (LPA). LPA is further converted into phosphatidic acid (PA), a precursor of triacylglycerol and membrane phospholipids, by LPA acyltransferases (LPAATs) which are localized in the ER membranes. Mammalian mitochondrial GPATs, GPAT1 and GPAT2, correspond to *C. elegans* ACL-6. Mammalian microsomal GPATs, GPAT3 and GPAT4, correspond to *C. elegans* ACL-4 and ACL-5. *C. elegans* LPAATs are ACL-1 and ACL-2. (**B–D**) Genomic structures of ER-GPAT (*acl-4* and *acl-5*) (**B**), Mt-GPAT (*acl-6*) (**C**) and LPAAT (*acl-1* and *acl-2*) (**D**). Grey boxes indicate exons and white boxes indicate 5′ and 3′ untranslated regions. The extent of deletion in *acl-4(xh10)*, *acl-5(xh19)*, *acl-6(tm3396* and *tm3452)*, *acl-1(tm3289)*, and *acl-2(tm3246)* are indicated by horizontal double arrows. The positions of the predicted conserved lysophospholipid acyltransferase motifs, characteristic of AGPAT family members, are shown in yellow lines. (**E**) GPAT activity in the membrane fractions of wild-type and the indicated *acl* mutants. [^{14}C]Palmitoyl-CoA (40 µM) and glycerol-3-phosphate (G3P) (800 µM) were used. We could not measure GPAT activity of the worms lacking both ER-GPAT and Mt-GPAT double mutants (*acl-6;acl-4 acl-5* triple mutants) because they were lethal. (**F**) Triacylglycerol contents of wild-type and the indicated *acl* mutants. (**G**) Incorporation of [^{14}C]palmitic acids into neutral lipid fractions of the living worms. The amount of incorporation was expressed as the percentage of radioactivity incorporated into total lipids. (**H**) Phospholipids contents of wild-type and the indicated *acl* mutants. Each bar represents the mean ± s.e.m. of at least three independent experiments. $^{*}P<0.05$, $^{**}P<0.01$, $^{***}P<0.001$ (Student's *t* test).

question, a comprehensive mutational analysis of GPATs would be useful. The *C. elegans* genome contains two microsomal GPATs (*acl-4*, *acl-5*), and one mitochondrial GPAT (*acl-6*) (Figure 1A). To understand the functional differences of the two types of GPAT, we generated *C. elegans* deletion mutants of mitochondrial and microsomal GPATs.

Mitochondria are essential organelles in most eukaryotic cells that are involved in several metabolic pathways, cell signalling, and apoptosis. Mitochondria undergo dynamic changes in morphology through continual fission and fusion, which is essential for maintenance of mitochondrial function and to adapt mitochondria to cellular needs

(Detmer and Chan, 2007). The balance of fission and fusion determines the overall mitochondrial morphology. When mitochondrial fusion is reduced, mitochondria fragment due to ongoing fission; conversely, mitochondria are long and overly interconnected when this balance shifts towards fusion (Smirnova *et al*, 1998, 2001; Chen *et al*, 2003; Eura *et al*, 2003; Santel *et al*, 2003). Genetic studies in *D. melanogaster* and *S. cerevisiae* have led to the identification of components that regulate mitochondrial dynamics (Okamoto and Shaw, 2005; Westermann, 2008; Hoppins and Nunnari, 2009). These include the mitofusin (Mfn), which is involved in mitochondrial fusion, and Drp1, which is involved in mitochondrial fission. Mfn is a large transmembrane GTPase localized in the mitochondrial outer membrane (Santel and Fuller, 2001; Rojo *et al*, 2002; Chen *et al*, 2003; Eura *et al*, 2003; Santel *et al*, 2003; Ishihara *et al*, 2004), whereas Drp1 is a cytosolic dynamin-related GTPase that is associated with the mitochondrial outer membrane at sites of fission (Smirnova *et al*, 1998, 2001). These molecules are evolutionarily conserved in eukaryotic organisms including human and *C. elegans*.

Here, we show that depletion of mitochondrial GPAT in *C. elegans* causes mitochondrial fragmentation. This defect is most probably induced by impaired mitochondrial fusion. We also demonstrate that injection of LPA, a direct product of GPAT, into cells rescues the mitochondrial defect in the mitochondrial GPAT mutants. We propose, from these results, that in addition to functioning as a precursor of glycerolipid synthesis, LPA produced by mitochondrial GPAT plays an important role in regulating mitochondrial dynamics.

Results

Identification of microsomal and mitochondrial GPAT in C. elegans

A search of the *C. elegans* genome for proteins with four conserved AGPAT motifs yielded 14 proteins (*acl-1-14*) (Imae *et al*, 2010). Among these genes, *acl-4* and *acl-5* are homologous to microsomal GPATs (GPAT3 and GPAT4) and show 45–60% identity to human GPAT3 and GPAT4 (Figure 1A; Supplementary Figure S1A). *acl-6* is a sole *C. elegans* homologue of mitochondrial GPATs (GPAT1 and GPAT2) and shows about 30% identity to human GPAT1 and GPAT2 (Figure 1A; Supplementary Figure S1B). As expected from the sequence homology, *acl-4* and *acl-5* gene products colocalized with an ER marker (calnexin) (Supplementary Figure S2A–F), but not with a mitochondrial marker (MitoTracker) (Supplementary Figure S2J–O) when expressed in mammalian cells. In contrast, the *acl-6* gene product colocalized with a mitochondrial marker in mammalian cells (Supplementary Figure S2P–R) and also in *C. elegans* muscle cells (Supplementary Figure S2S–U).

Generation of GPAT mutants

To address the *in vivo* functions of LPA-producing enzymes, we isolated deletion mutants of all GPATs by PCR-based screening of UV-TMP-mutagenized libraries. The *acl-4(xh10)* allele had a deletion that causes a frameshift resulting in a premature stop codon (Figure 1B). The *acl-5(xh19)* allele lacked the translation initiation codon (Figure 1B). Both alleles lacked the conserved AGPAT motifs that are essential for enzyme activity. Two deletion alleles of *acl-6, tm3396,* and *tm3452,* caused a frameshift leading to a premature stop codon (Figure 1C). Both *tm3396* and *tm3452* appeared to be null or strong loss-of-function alleles because inhibition of *acl-6* by RNAi failed to enhance the *acl-6* mutant phenotypes described below. Because *acl-6(tm3396)* and *acl-6(tm3452)* were phenotypically indistinguishable, we used *acl-6(tm3396)* mutants in subsequent experiments.

In *acl-4 acl-5* double mutants (hereafter, referred to as 'ER-GPAT mutants'), GPAT activity in the membrane fraction was reduced to 25% of the level in the wild type (Figure 1E) and the triacylglycerol level was reduced to 46% of the level in the wild type (Figure 1F). Incorporation of supplemented [^{14}C]palmitic acid into the triacylglycerol fraction was also reduced in ER-GPAT mutants (Figure 1G). In contrast, no reductions in GPAT activity, the triacylglycerol level, or incorporation of [^{14}C]palmitic acid into triacylglycerol were observed in *acl-6* mutants ('Mt (mitochondrial)-GPAT mutants') (Figure 1E–G). However, in the ER-GPAT mutant background, knockdown of Mt-GPAT significantly reduced the incorporation of [^{14}C]palmitic acid into triacylglycerol (Figure 1G). These data indicate that ER-GPAT and Mt-GPAT complement each other to maintain triacylglycerol synthesis in *C. elegans*.

On the other hand, the amount of phospholipids, the other final products of glycerolipid synthesis, was not affected in either ER-GPAT mutants or Mt-GPAT mutants (Figure 1H). Mutants lacking both mitochondrial and microsomal GPATs (*acl-6; acl-4 acl-5* triple mutants) did not survive (Table I; Supplementary Table S1A, see Materials and methods for details).

Mitochondrial GPAT, acl-6, is required for oogenesis in C. elegans

Single mutants with *acl-4* or *acl-5*, and *acl-4 acl-5* double mutants (ER-GPAT mutants) were viable and showed no detectable abnormalities in viability, growth, morphology, or motility under a dissecting microscope (Table I, ER-GPAT mutants). In contrast, 18% of *acl-6* mutants (Mt-GPAT mutants) died during late embryogenesis (Table I, Mt-GPAT mutants, Emb). Hatched Mt-GPAT mutants developed normally to the adult stage; however, about 70% of these animals were sterile (Table I, Mt-GPAT mutants, Ste). The embryonic lethality and sterility of Mt-GPAT mutants were efficiently rescued by expression of *acl-6* cDNA under the control of its own promoter (Table I, *acl-6(tm3396); Ex[Pacl-6::acl-6::gfp]*).

We then focused on the reproductive system of Mt-GPAT mutants. The gonadal arm of the adult hermaphrodite is U shaped, with a distal arm composed of a syncytium of germline nuclei and a proximal arm containing oocytes and fertilized eggs (Figure 2A; Hubbard and Greenstein, 2005; Kimble and Crittenden, 2005). Germ cells proliferate mitotically in the distal-most region, and as they migrate proximally, they enter meiotic prophase in the transition zone (Hubbard and Greenstein, 2005; Kimble and Crittenden, 2005). In Mt-GPAT mutants, the U-shaped gonad was reduced in size and contained no oocytes in the proximal position, while the morphology of the vulva, an egg-laying apparatus, appeared normal (Figure 2B). DAPI staining of

Table I Phenotypic consequences of *C. elegans* GPAT and LPAAT mutants

Strain	Emb (%)	Larval arrest (%)	Ste (%)[a]	Brood size
Wild type	<1	<1	0	326 ± 22 ($n = 20$)
ER-GPAT mutants				
acl-4(xh10)	<1	<1	0	286 ± 29 ($n = 20$)
acl-5(xh19)	<1	<1	0	323 ± 24 ($n = 20$)
acl-4(xh10) acl-5(xh19)	<1	<1	0	303 ± 21 ($n = 20$)
Mt-GPAT mutants				
acl-6(tm3396)	18.0 ($n = 649$)	<1	74.0 ($n = 169$)	141 ± 80[b] ($n = 20$)
acl-6(tm3452)	16.9 ($n = 767$)	<1	64.3 ($n = 185$)	66 ± 39[b] ($n = 20$)
acl-6(tm3396); Ex[Pacl-6::acl-6::gfp]	3.8 ($n = 394$)	<1	2.7 ($n = 74$)	172 ± 70[b] ($n = 20$)
ER and Mt-GPAT mutants				
acl-6(tm3396); acl-4(xh10) acl-5(xh19)	100[c](Emb + larval arrest)		ND	ND
LPAAT mutants				
acl-1(tm3289)	<1	<1	0	309 ± 32 ($n = 20$)
acl-2(tm3246)	<1	<1	0	298 ± 50 ($n = 18$)
acl-2(tm3246); acl-1(tm3289)	100[c](Emb + larval arrest)		ND	ND
ER-GPAT-LPAAT mutants				
acl-4(xh10) acl-5(xh19) acl-1(tm3289)	6.4 ($n = 299$)	<1	0	293 ± 30 ($n = 20$)
acl-2(tm3246); acl-4(xh10) acl-5(xh19)	4.2 ($n = 528$)	<1	0	304 ± 45 ($n = 19$)
Mt-GPAT-LPAAT mutants				
acl-6(tm3396); acl-1(tm3289)	13.1 ($n = 727$)	<1	31.7 ($n = 145$)	160 ± 101[b] ($n = 20$)
acl-2(tm3246) acl-6(tm3396)	19.2 ($n = 266$)	<1	51.3 ($n = 150$)	143 ± 86[b] ($n = 20$)

All strains were raised at 20°C.[a]Worms were scored as sterile if no eggs were produced.
[b]Average brood size of worms producing more than one egg. Note that complete sterile worms were excluded from the count.
[c]Triple mutation of GPAT (*acl-4, acl-5*, and *acl-6*) and double mutation of LPAAT *(acl-1* and *acl-2*) were synthetic lethal including embryonic lethal and early larval arrest. Also see the Supplementary Table.

Mt-GPAT mutants also revealed a reduction in the number of germ cells in the mitotic and transition zone and an absence of oocytes at the diakinesis stage (Figure 2C and D). These data indicate that mitochondrial GPAT, *acl-6*, is required for normal oogenesis.

Deletion of Mt-GPAT causes abnormal mitochondrial morphology

We next examined the mitochondrial morphology of Mt-GPAT mutants by staining with MitoTracker. In wild-type gonads, a meshwork-like structure of mitochondria was observed around the germ cell nuclei (Figure 3A), as reported previously (Labrousse *et al*, 1999; Pitt *et al*, 2000). In Mt-GPAT mutant gonads, a meshwork-like structure was lost and the MitoTracker staining was faint (Figures 3B and 4I). Thin-section transmission electron microscopy (TEM) revealed that Mt-GPAT mutants lacked mitochondria with normal morphology, but had swollen and abnormal structures that were not present in wild-type gonads (Figure 3E and F, white arrowhead). Because impaired mitochondrial function causes sterility in *C. elegans* (Artal-Sanz *et al*, 2003; Bratic *et al*, 2009), mitochondrial abnormality in the Mt-GPAT mutants may lead to sterility at the adult stage.

In the wild type, muscle cell mitochondria were tubular and elongated and ran parallel to the myofibrils as previously reported (Figure 3C; Labrousse *et al*, 1999), while in the Mt-GPAT mutants, they were fragmented and disorganized (Figures 3D and 4J). We also examined the mitochondrial morphology in Mt-GPAT mutants by expressing mitoGFP in the wall muscle cells. Mitochondria observed with mitoGFP, like those observed with MitoTracker, were significantly fragmented in Mt-GPAT mutants (Supplementary Figure S3). The mitoGFP fluorescence mostly matched the Mitotracker stain, indicating that fragmented mitochondria still maintain membrane potential. MitoGFP also detected very small portions of mitochondria that were not detected by Mitotracker (Supplementary Figure S3, arrowhead). TEM analysis showed that mitochondria of the Mt-GPAT mutants were short and round (Figure 3H, arrowheads), whereas those of wild-type muscle were long and tubular (Figure 3G, arrows). We measured the rates of thrashing, readouts for muscle activity, and found that the Mt-GPAT mutation reduced thrashing rates by 78% compared to the wild type (Supplementary Figure S4).

We conducted cell-specific rescue experiments to confirm the cell autonomy of Mt-GPAT (*acl-6*) function. The fragmented mitochondria in muscle cells were rescued by expression of *acl-6* in the muscle cells (under *myo-3* promoter), but not by expression in the intestine cells (under *ges-1* promoter) (Supplementary Figure S5A–C), indicating that *acl-6* functions cell autonomously to maintain mitochondrial morphology.

Next, we determined whether GPAT activity of Mt-GPAT is required for maintaining mitochondrial morphology. Essential amino-acid residues for the catalytic activity have been identified in mammalian GPAT1 (Dircks *et al*, 1999). Then, we generated transgenic worms expressing GFP-tagged human GPAT1 (*acl-6 [Pmyo-3::hgpat1 (WT)::GFP]*) or catalytically inactive hGPAT1 (arginine 318 to alanine; R318A) (*acl-6 [Pmyo-3::hgpat1 (R318A)::GFP]*). As shown in Figure 3K, the membrane fractions of HEK293 cells expressing hGPAT1 (R318A)-FLAG did not show increased GPAT activity compared with those of hGPAT1 (WT).

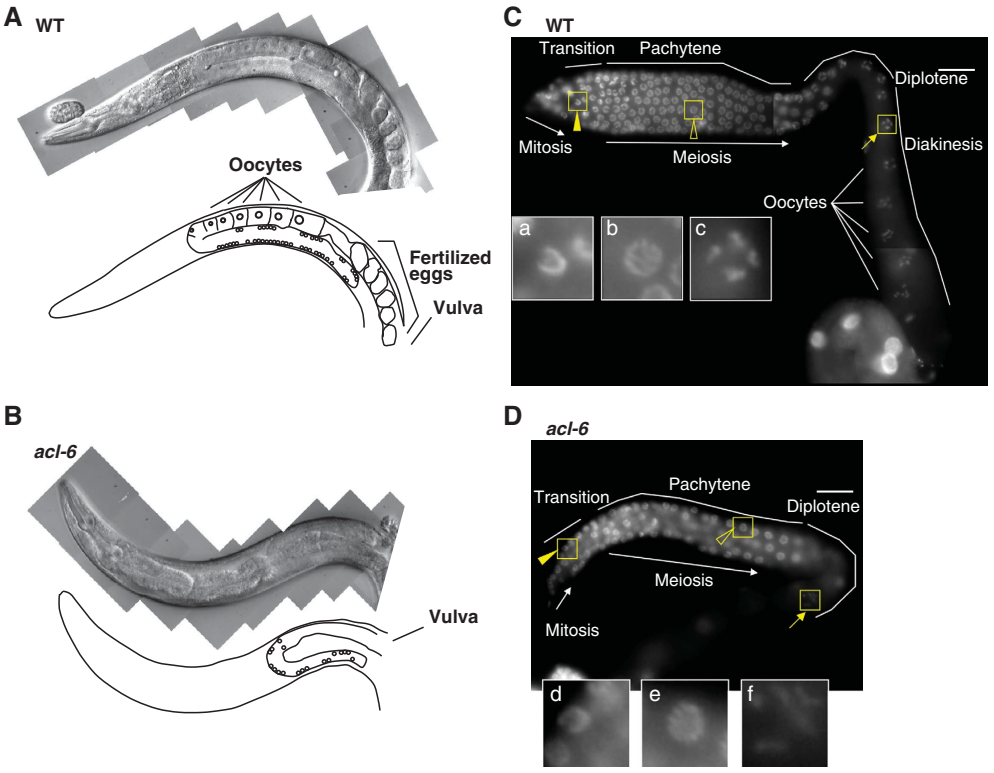

Figure 2 Mt-GPAT mutants show defects in oogenesis. (**A**, **B**) Nomarski images and schematic diagrams of the adult hermaphrodite gonads of wild-type (**A**) and Mt-GPAT (*acl-6)* mutant (**B**). (**C**, **D**) DAPI-stained images of adult hermaphrodite gonads of wild-type (**C**) and Mt-GPAT (*acl-6)* mutant (**D**). (Insets) Enlargement of the boxed regions: transition states (a, d), pachytene nuclei (b, e), diplotene nuclei (f), and diakinesis nuclei (c). Scale bars, 20 μm.

Mitochondrial fragmentation in Mt-GPAT mutants was rescued in hGPAT1 (WT)-expressing cells (Figure 3I), but not in hGPAT1 (R318A)-expressing cells (Figure 3J). Thus, GPAT activity of Mt-GPAT is required for normal mitochondrial morphology.

LPA is required for normal mitochondrial morphology

The finding that GPAT activity was required for normal mitochondrial morphology indicated that LPA, a product of GPAT, or the downstream metabolites in glycerolipids synthesis pathway is involved in mitochondrial morphology. Then, we conducted RNAi knockdown of 80 genes whose homologues are reported to be involved in phospholipid synthesis and lipid transfer in other species (Supplementary Table S2) in Mt-GPAT (*acl-6*) mutants. Interestingly, we found that inhibition of *acl-1* rescued the sterility (Figure 4A–C) and abnormal mitochondrial morphology (Figure 4E–J). *acl-1* encodes a homologue of mammalian LPAAT, which catalyses the conversion of LPA to PA (Figure 1A; Supplementary Figure S1C). The *acl-1* mutation reduced LPAAT activity to 17% of that in the wild type (Figures 1D and 4D), and caused no detectable abnormalities (Table I, LPAAT mutants). The *acl-1* mutation rescued both abnormal MitoTracker staining in the gonad and abnormal mitochondrial morphology in muscle cells of Mt-GPAT mutants (Figure 4E, F, I and J). TEM analysis also showed that *acl-1* mutation restored normal mitochondrial morphology in Mt-GPAT mutants (Figure 4G and H). Two human LPAAT isoforms have been cloned (Figure 1A), and we identified *acl-2* as another homologue of mammalian LPAAT. Although the *acl-2* mutation did not significantly reduce the *in vitro* LPAAT activity (Figures 1D and 4D), double mutations of *acl-1* and *acl-2* resulted in lethal phenotypes (Table I; Figure 1D; Supplementary Table S1B), suggesting that *acl-1* and *acl-2* cooperatively function as LPAAT. The *acl-2* mutation also rescued the sterility of Mt-GPAT mutants, but to a lesser extent than did the *acl-1* mutation (Figure 4C).

Since reduction in LPAAT activity is assumed to increase the level of LPA in the cells by suppressing the conversion of LPA to PA (Figure 1A), we hypothesized that an increased level of LPA, a direct product of GPAT reaction, could rescue the mitochondrial defects of Mt-GPAT mutants. To test this hypothesis, we injected LPA directly into the gonad of Mt-GPAT mutants. When a solution is injected into the *C. elegans* gonad, it spreads within the cytoplasm and directly reaches the organelles of germ cells because the gonad is a syncytium where germ nuclei share the cytoplasm (Hubbard and Greenstein, 2005). About 80% of non-treated or vehicle-injected Mt-GPAT mutants showed faint MitoTracker staining in the gonad (Figure 5A and J). By injection of 1-palmitoyl-2-hydroxy-*sn*-glycerol-3-phosphate, a molecular species of LPA, into the gonad, about half of the Mt-GPAT mutants showed normal meshwork-like MitoTracker staining (Figure 5B and J). Injection of other lysophospholipids such as lysophosphatidylcholine and lysophosphatidylserine did not rescue the abnormal mitochondrial staining (Figure 5C, D, and J). Since LPA is a metabolically active intermediate of glycerolipid synthesis, it can be hydrolysed at the bond between phosphate and the glycerol backbone to form monoacylglycerol, or it can be acylated at the *sn*-2 position

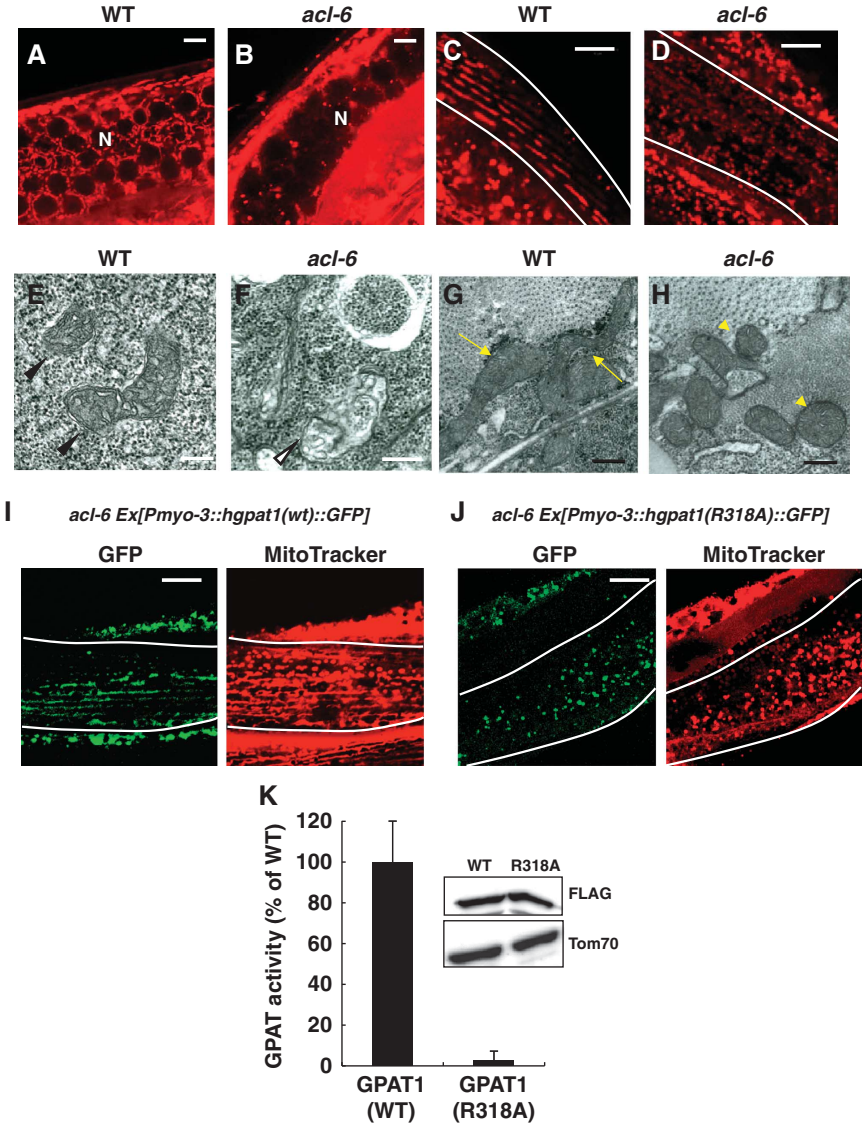

Figure 3 Mt-GPAT deficiency causes defects in mitochondrial morphology. (**A**, **B**) MitoTracker staining of germ cells in wild-type (**A**) and Mt-GPAT (*acl-6)* mutant (**B**). N: nuclei. Scale bars, 5 μm. (**C**, **D**) MitoTracker staining of wild-type (**C**) and Mt-GPAT (*acl-6)* mutant (**D**). Body wall muscle cells are outlined with lines. Scale bars, 10 μm. (**E**, **F**) Transmission electron micrographs of germ cells in wild-type (**E**) and Mt-GPAT (*acl-6)* mutant (**F**). Arrowheads indicate the mitochondria with normal morphology. A white arrowhead indicates a swollen and abnormal mitochondrial-like structure. Scale bars, 200 nm. (**G**, **H**) Transmission electron micrographs of body wall muscle cells in wild-type (**G**) and Mt-GPAT (*acl-6)* mutant (**H**). Arrows indicate long and tubular mitochondria and arrowheads indicate short and round mitochondria. Scale bars, 200 nm. (**I**, **J**) Mt-GPAT (*acl-6*) mutants expressing hGPAT1 (WT):: GFP (**I**) or hGPAT1 (R318A):: GFP (**J**) translational fusion protein in body wall muscle cells using a *myo-3* promoter were stained with MitoTracker. Body wall muscle cells are outlined with lines. Scale bars, 10 μm. (**K**) Glycerol-3-phosphate acyltransferase (GPAT) activity in the membrane fractions of HEK293 cells expressing hGPAT1(WT)-FLAG or hGPAT1(R318A)-FLAG. [^{14}C]Palmitoyl-CoA (40 μM) and glycerol-3-phosphate (G3P) (800 μM) were used. Activities of mutant forms are expressed as percentages of wild-type activity. The values represent the mean ± s.e.m. of four independent experiments. The insets show immunoblots of HEK 293 cells expressing GPAT1(WT)-FLAG or GPAT1(R318A)-FLAG after fractionation into membrane fraction.

to form PA. However, these metabolites did not rescue the mitochondrial staining (Figure 4E, F, and J). We also injected metabolically stabilized LPA analogues such as 1-oleoyl-2-*O*-methyl-glycerophosphothionate (OMPT), XY-26, and XY-47 (Supplementary Figure S6B–E; Xu *et al*, 2005). OMPT, in which the hydroxy group and the phosphate are converted to an *O*-methoxy group and a phosphothionate, is an acyltransferase- and phosphatase-resistant analogue. XY-26 is a phosphatase-resistant LPA analogue in which the bridging oxygen in the mono phosphate is replaced by an α-monofluoromethylene (-CF-) moiety. XY-47 is an alkyl LPA in which the *sn*-1 *O*-acyl group is replaced by an *O*-alkyl ether, and is resistant to phospholipase A. We found that all these LPA analogues suppressed the mitochondrial defects (Figure 6G–J). Although these LPA analogues may have ability to suppress LPAAT activity, which also rescues the mitochondrial defects in Mt-GPAT mutants (see Figure 4E), we found that these analogues did not inhibit LPAAT activity (Supplementary Figure S6A). These results, together with the genetic rescue by the LPAAT mutation, strongly suggest that LPA is required for normal mitochondrial morphology.

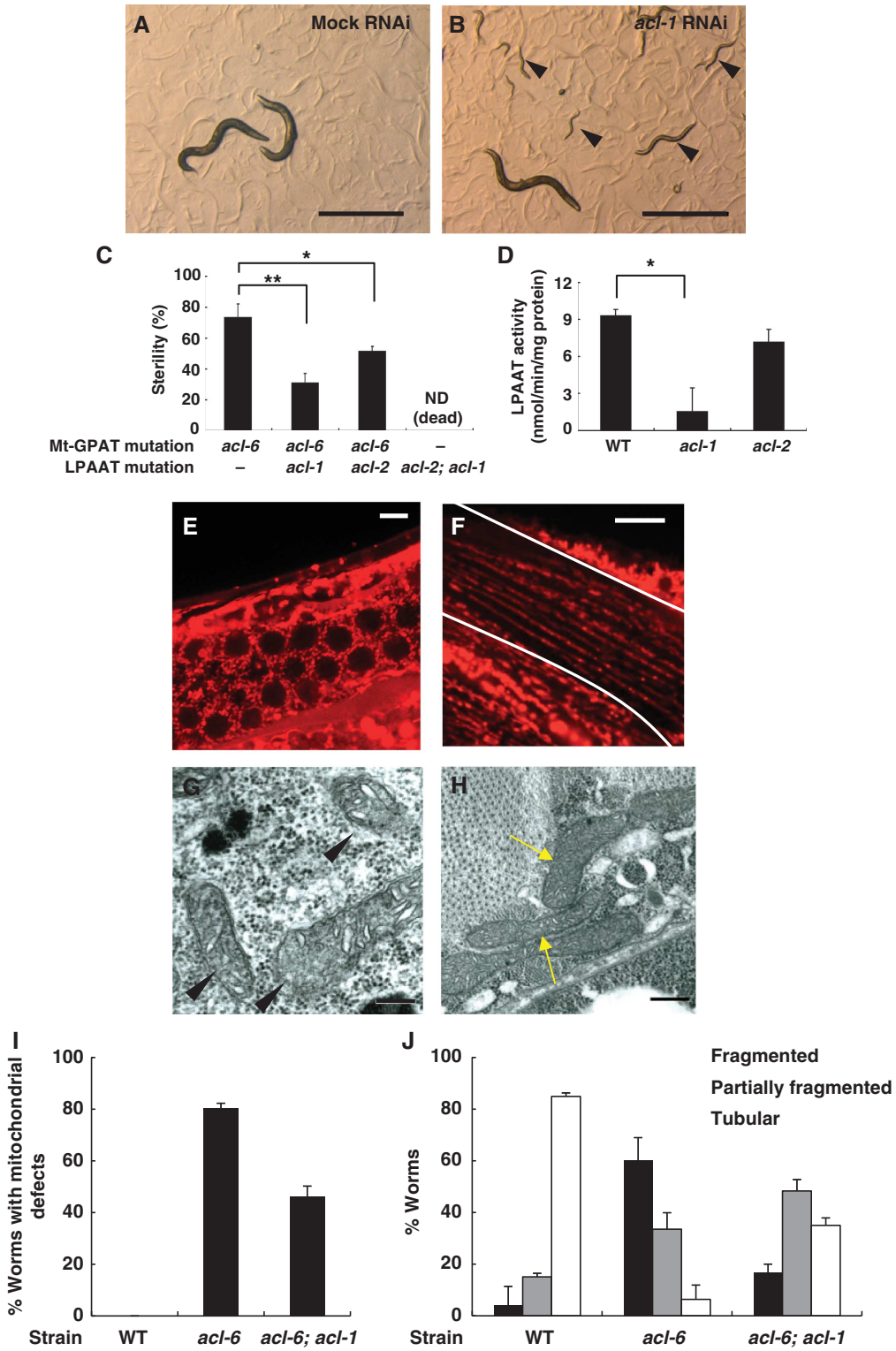

Figure 4 Mitochondrial defects of Mt-GPAT mutants are suppressed by LPAAT (*acl-1*) mutation. (**A**, **B**) Photographs of Mt-GPAT (*acl-6*) mutants subjected to mock (**A**) or *acl-1* RNAi (**B**). Note that Mt-GPAT (*acl-6*) mutants produced progeny when they were subjected to *acl-1* RNAi (arrowheads). Scale bars, 1 mm. (**C**) The percentage of sterile worms in each strain. *acl-2; acl-1* double mutants that lack both LPAATs were lethal. Each bar represents the mean ± s.e.m. of at least three independent experiments ($n > 50$ for each experiment). $^{*}P < 0.05$, $^{**}P < 0.01$ (Student's *t* test). (**D**) LPA acyltransferase activity in the membrane fractions of wild-type, *acl-1* mutants, and *acl-2* mutants. 1-oleoyl lysophosphatidic acid (40 μM) and [^{14}C]oleoyl-CoA (12.5 μM) were used. Each bar represents the mean ± s.e.m. of at least three independent experiments. $^{*}P < 0.05$ (Student's *t*-test). (**E**, **F**) MitoTracker staining of germ cells (**E**) and body wall muscle cells (**F**) in *acl-6; acl-1* double mutants. Body wall muscle cells are outlined with lines. Scale bars, 5 μm (germ cells) and 10 μm (muscle cells). (**G**, **H**) Transmission electron micrographs of germ cells (**G**) and body wall muscle cells (**H**) in *acl-6; acl-1* double mutants. Arrowheads indicate the mitochondria with normal morphology and arrows indicate long and tubular mitochondria. Scale bars, 200 nm. (**I**) The percentage of worms with mitochondrial defects in germ cells evaluated by MitoTracker stain. The experiment was repeated three times ($n > 20$ for each experiment). Bars, mean ± s.e.m. (**J**) The bar graph shows the relative frequencies of worms with fragmented, partially fragmented or tubular mitochondria in each strain. The experiment was repeated three times ($n > 20$ for each experiment). Bars, mean ± s.e.m.

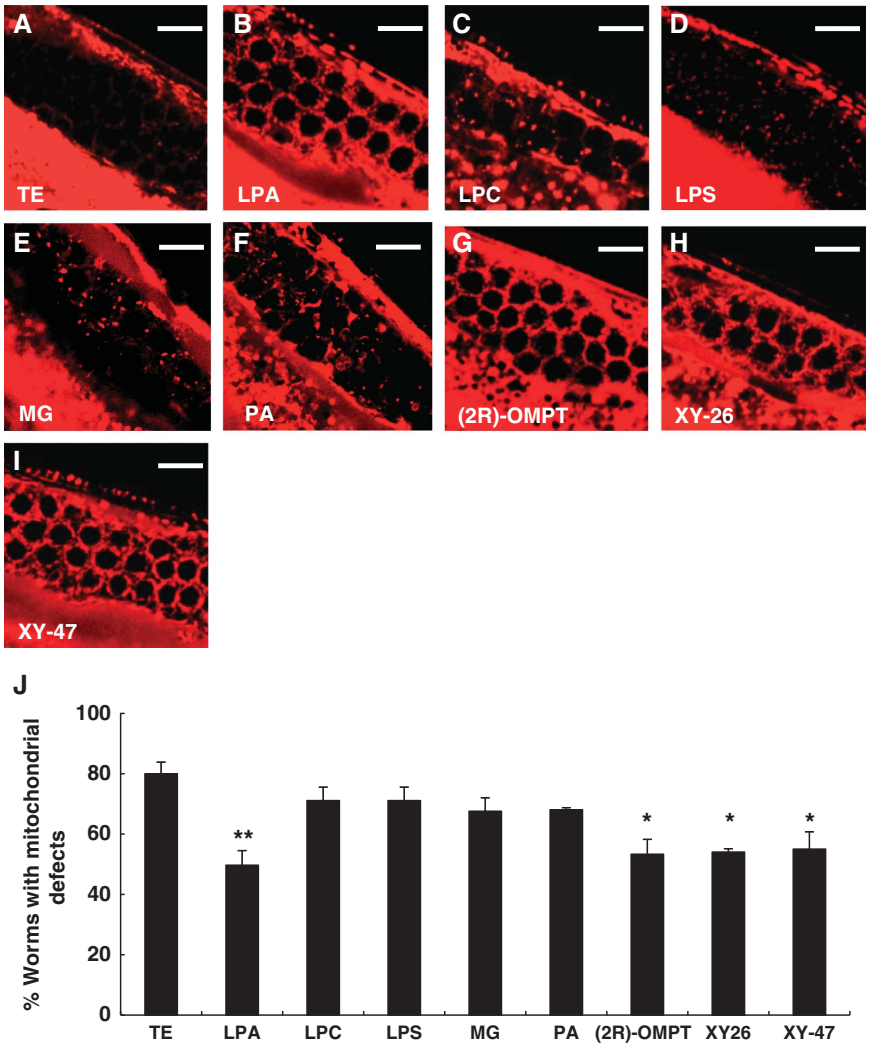

Figure 5 Injection of LPA into germ cells suppresses the mitochondrial defects in Mt-GPAT mutants. (**A–I**) Mt-GPAT (*acl-6)* mutants were injected with each lipid into the gonad, and stained with MitoTracker. Germ cells stained with MitoTracker are shown. Scale bars, 10 μm. (**J**) The percentage of worms with mitochondrial defects in germ cells. The experiment was repeated three times ($n > 20$ for each experiment). Bars, mean ± s.e.m. $^{*}P < 0.05$, $^{**}P < 0.01$ (Student's *t*-test compared to TE injection).

Abnormal mitochondrial morphology in Mt-GPAT mutants is suppressed by drp-1 RNAi

Proper mitochondrial morphology results from a balance between fission and fusion, which compete against each other (Sesaki and Jensen, 1999; Hoppins and Nunnari, 2009). Mitochondrial fragmentation that we observed in Mt-GPAT mutant muscle cells (Figure 3D and H) led us to hypothesize that Mt-GPAT inhibition reduces fusion. Studies in *S. cerevisiae* and mammals have demonstrated that defects in mitochondrial fusion can be ameliorated by mutations in genes required for mitochondrial fission and *vice versa*. We knocked down the expression of the pro-fission protein Drp1 in Mt-GPAT mutants. As a control, we checked mitochondrial morphology in mutants of a pro-fusion protein Mfn (*fzo-1* mutants). The *fzo-1* mutation caused fragmented mitochondria in the muscle cells, which was suppressed by *drp-1* RNAi (Supplementary Figure S7A and B), as reported previously (Ichishita *et al*, 2008). The *fzo-1* mutation also reduced MitoTracker staining in the gonad, which was recovered by *drp-1* RNAi (Supplementary Figure S7C and D). In Mt-GPAT mutants, *drp-1* RNAi significantly suppressed both fragmented mitochondria of muscle cells and MitoTracker staining of the gonad (Figure 6A–E). Furthermore, overexpression of *fzo-1* suppressed the fragmented mitochondria of muscle cells in Mt-GPAT mutants (Figure 6F–I). These results indicate that Mt-GPAT inhibition reduces fusion and/or enhances fission, leading to abnormal mitochondrial morphology. *drp-1* RNAi did not rescue significantly the oogenesis defect of Mt-GPAT mutants (Supplementary Figure S8). Although mitochondrial morphology is apparently rescued by *drp-1* RNAi, mitochondrial function may not be restored enough to rescue the fertility. Alternatively, LPA produced by Mt-GPAT may have an as yet unknown function in oogenesis.

Although *acl-1* mutation, which may raise the intracellular LPA level, rescued mitochondrial fragmentation caused by *fzo-1* RNAi (Figure 6J–L), it did not rescue mitochondrial fragmentation caused by *fzo-1* mutation (Supplementary Figure S7E), suggesting that LPA acts on the *fzo-1*-dependent mitochondrial fusion.

Knockdown of Mt-GPAT leads to mitochondrial fragmentation in HeLa cells

To determine whether Mt-GPAT is required for mitochondrial morphology in mammals, we used HeLa cells in which

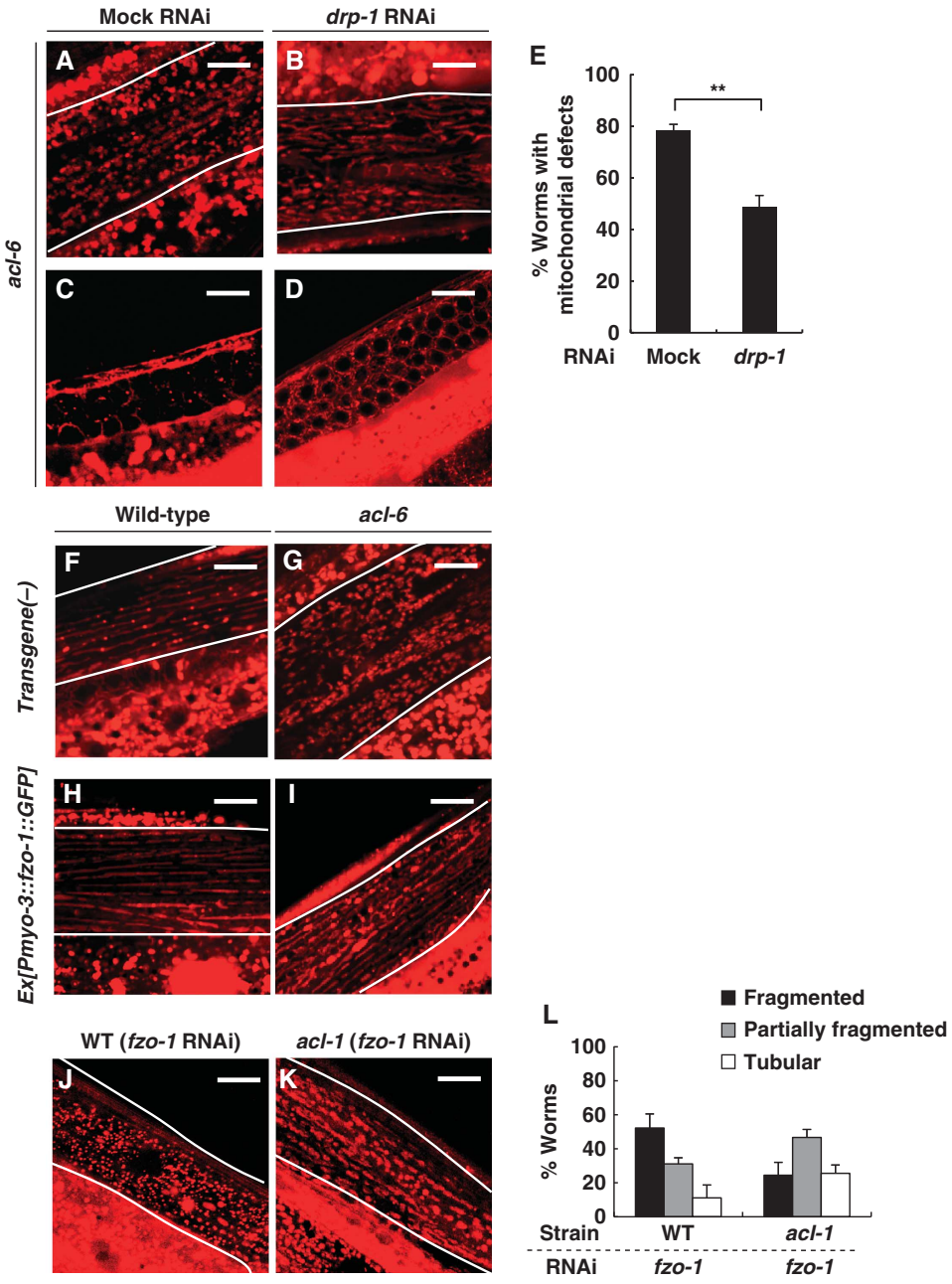

Figure 6 Inhibition of Drp1 rescues the mitochondrial defects in Mt-GPAT mutants. (**A**–**D**) MitoTracker staining of body wall muscle cells (**A**, **B**) and germ cells (**C**, **D**) in Mt-GPAT (*acl-6)* mutants subjected to mock or *drp-1* RNAi. Body wall muscle cells are outlined with lines. Scale bars, 10 μm. (**E**) The percentage of worms with the mitochondrial defects in germ cells evaluated by MitoTracker stain. Each bar represents the mean ± s.e.m. of three independent experiments ($n > 20$ for each experiment). $^{**}P < 0.01$ (Student's *t*-test). (**F**–**I**) MitoTracker staining of body wall muscle cells in wild-type (**F**, **H**) and Mt-GPAT (*acl-6)* mutants (**G**, **I**) expressing the *C. elegans* mitofusin homologue, FZO-1. FZO-1::GFP was specifically expressed in body wall muscle cells using a *myo-3* promoter. Body wall muscle cells are outlined with lines. Scale bars, 10 μm. (**J**–**L**) MitoTracker staining of body wall muscle cells in wild-type (**J**) or *acl-1* mutants (**K**) subjected to *fzo-1* RNAi. Body wall muscle cells are outlined with lines. Scale bars, 10 μm. The bar graph shows the relative frequencies of worms with fragmented, partially fragmented or tubular mitochondria in each strain. The experiment was repeated three times ($n > 30$ for each experiment). Bars, mean ± s.e.m. (**L**).

GPAT1 was a major mitochondrial GPAT isoform (Supplementary Figure S9A). In cells transfected with GPAT1 siRNA duplex, the GPAT1 mRNA level was reduced to 24% of the level in control siRNA-transfected cells at 72 h after transfection (Supplementary Figure S9B). In control cells, mitochondria visualized by MitoTracker were characterized by a network of extended wavy tubules throughout the cytoplasm (Figure 7A). In contrast, mitochondria appeared as punctate structures in GPAT1-depleted cells (Figure 7B). In electron micrographs, mitochondrial networks appeared to be collapsed to form small and fragmented mitochondria in GPAT1-depleted cells, while mitochondria were long and tubular in control cells (Figure 7C and D). Quantitative analysis of electron micrographs revealed that the mitochondrial aspect ratio was smaller in GPAT1-depleted cells than in control cells (Figure 7E). The mitochondrial membrane potential and the ratio of mitochondrial DNA: nuclear DNA were not changed in GPAT1-depleted cells (Supplementary

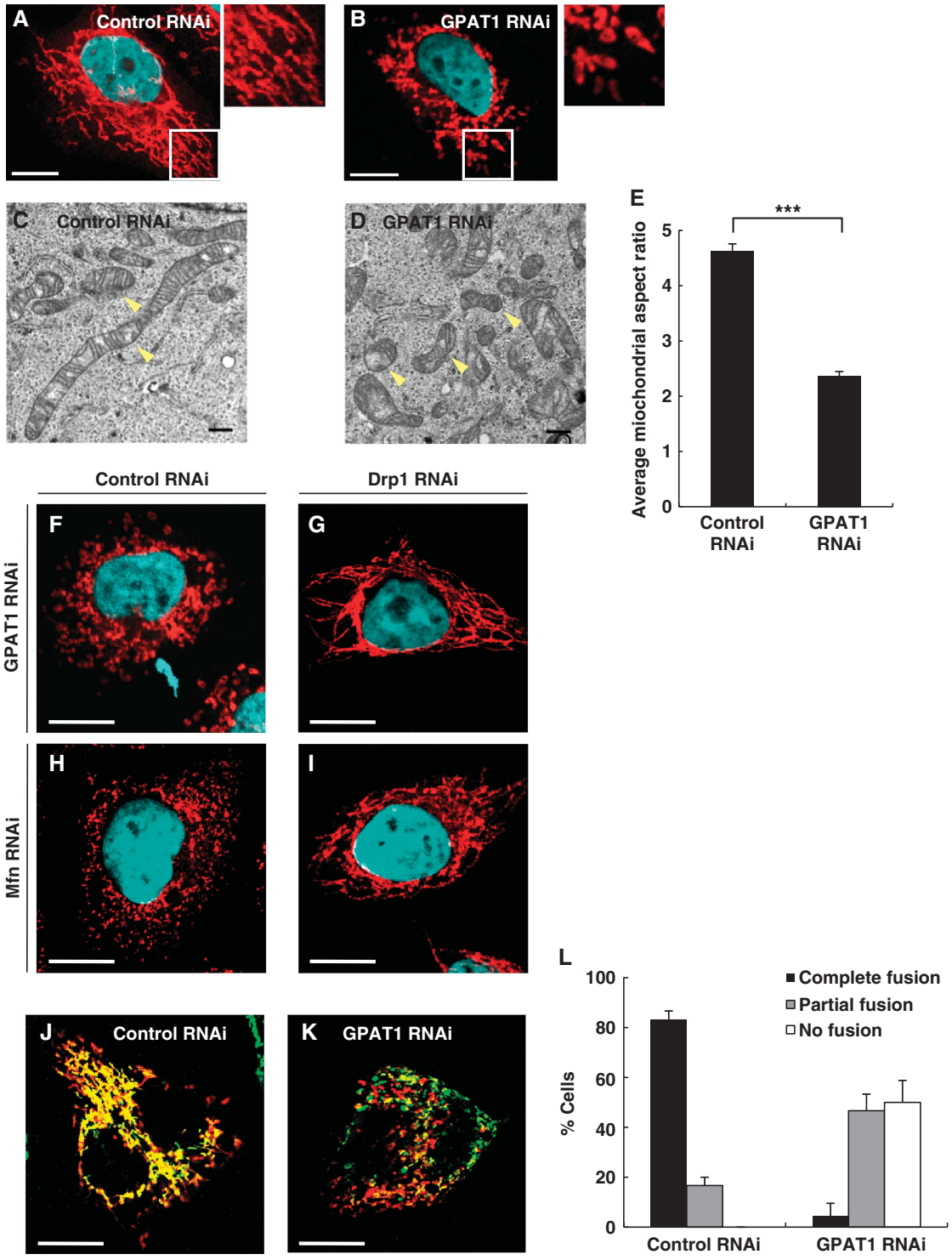

Figure 7 Mt-GPAT is required for mitochondrial fusion in HeLa cells. (**A**, **B**) HeLa cells were transfected with control (**A**) or Mt-GPAT (GPAT1) siRNA (**B**), and stained with MitoTracker and DAPI. White boxes indicate regions enlarged in insets. Scale bars, 10 μm. (**C**, **D**) Transmission electron micrographs of HeLa cells, transfected with control (**C**) or Mt-GPAT (GPAT1) siRNA (**D**). Arrowheads indicate mitochondria. Scale bars, 500 nm. (**E**) Mitochondrial length was determined by analysing the aspect ratio (length of major axes/minor axes). Data are shown as mean ± s.e.m. $***P<0.001$ (Student's *t*-test). (**F**–**I**) HeLa cells were treated with siRNA against the indicated genes and stained with MitoTracker and DAPI. Scale bars, 10 μm. (**J**–**L**) HeLa cells expressing su9-GFP or su9-RFP (Taguchi *et al*, 2007) were coplated, fused with PEG1500 and imaged after 8 h. Confocal images of representative cells transfected with control (**J**) or Mt-GPAT (GPAT1) siRNA (**K**). Scale bars, 20 μm. The bar graph shows the relative frequencies of full, partial, and almost no fusion for each siRNA-treated cell. The experiment was repeated three times. Bars, mean ± s.e.m. (**L**).

Figure S9C and D). These results suggest that mitochondrial fragmentation in GPAT1-depleted cells was not caused by a loss of mitochondrial function.

Mitochondrial fragmentation in GPAT1-depleted cells was suppressed by knockdown of either Drp1 or LPAATs (LPAAT1 and LPAAT2) as it was in *C. elegans* Mt-GPAT mutants

(Figure 7F–I; Supplementary Figure S10). To address whether the fragmented mitochondria are the result of reduced fusion of mitochondria, we performed a mitochondrial fusion assay by using a cell fusion technique with polyethylene glycol (PEG) (Chen *et al*, 2003). When cells expressing mitochondrially targeted GFP were fused with cells expressing mitochondrially targeted RFP by using PEG, most of the fused cells contained extensively fused mitochondria as demonstrated by colocalization of green and red fluorescent signals (Figure 7J). In contrast, GPAT1-depleted cells showed reduced mitochondrial fusion activity, that is, 50% of fused cells possessed predominantly unfused mitochondria and 47% showed partial fusion (Figure 7K and L). These results indicate that mitochondrial GPAT is required for mitochondria fusion in mammals as well as in *C. elegans*.

Discussion

Mt-GPAT and ER-GPAT are considered as the initial enzymes for glycerolipid synthesis. In this study, we generated both GPAT mutants using *C. elegans* to elucidate the functional difference between Mt-GPAT and ER-GPAT. Mutants lacking either Mt-GPAT or ER-GPAT could survive but mutants lacking both GPATs could not, indicating that these two GPATs complement each other for synthesizing glycerolipids such as phospholipids, which are essential components of biological membranes. In addition to a role in the synthesis of glycerolipids, we found that Mt-GPAT is required for normal mitochondrial dynamics in both *C. elegans* and mammals. Mt-GPAT mutants, but not ER-GPAT mutants, showed abnormal mitochondrial morphology. Mitochondrial fragmentation in Mt-GPAT mutants was rescued by wild-type GPAT but not by catalytically inactive GPAT. The mitochondrial defect was also rescued by injection of LPA, a direct product of Mt-GPAT. Furthermore, the mitochondrial defect in Mt-GPAT mutants was rescued by inhibition of LPAAT, which converts LPA to PA. In Mt-GPAT mutants, LPA is normally produced in the ER by ER-GPAT and is further acylated to form PA by LPAAT. When the LPAAT activity is inhibited by an LPAAT mutation, LPA may be accumulated in the ER and fluxed into the mitochondria, which leads to restoration of the mitochondrial defects in Mt-GPAT mutants.

Among mammalian four GPATs, knockout mice for mitochondrial GPAT1 (GPAT1$^{-/-}$ mice) have been reported (Hammond *et al*, 2007). Mitochondria obtained from the liver of GPAT1$^{-/-}$ mice are more sensitive to Ca^{2+}-induced mitochondrial permeability transition, a common marker of mitochondrial dysfunction, though mitochondrial morphology appears normal. In mammals, GPAT2, another mitochondrial GPAT, may function to produce LPA, which may account for the apparent normal mitochondrial morphology in GPAT1$^{-/-}$ mice. We expect that double knockout of GPAT1 and GPAT2 would induce a mitochondrial fragmentation as observed in HeLa cells.

LPA has been shown to act as an extracellular signalling molecule that evokes a wide variety of cellular processes including cell proliferation and migration, smooth muscle contraction, and actin stress fibre formation (van Meeteren and Moolenaar, 2007; Ye and Chun, 2010). These processes are exerted through interactions with a family of G protein-coupled receptors on the plasma membrane (Aoki *et al*, 2008; Ye and Chun, 2010). Extracellular LPA is produced either from lysophosphatidylcholine by a plasma phospholipase D, named autotaxin, or from PA by an extracellular phospholipase A_1 (Aoki *et al*, 2008; Ye and Chun, 2010). In the present study, we showed that LPA produced by Mt-GPAT functions at mitochondria in a cell-autonomous manner. First, the mitochondrial defect in muscle cells was rescued by muscle-specific expression of *acl-6* (Mt-GPAT), but not by expression in other tissues such as the intestine. Second, the same muscle-specific expression of Mt-GPAT failed to rescue the mitochondrial defect in the gonads (Supplementary Figure S5D–H). Third, Mt-GPAT RNAi caused sterility in the *rrf-1* mutant background, in which RNAi works only in the germ cells in the gonads (Supplementary Figure S5I–K; Sijen *et al*, 2001). These observations indicate that LPA produced by Mt-GPAT is an intracellular bioactive lipid that regulates mitochondrial morphology.

How does Mt-GPAT/LPA affect mitochondrial morphology? In this study, we provide three lines of evidence that Mt-GPAT/LPA is required for mitochondrial fusion. First, inhibition of Mt-GPAT caused mitochondrial fragmentation which is similar to that caused by inhibition of a pro-fusion protein, Mfn (mammals)/FZO-1 (*C. elegans*). Second, as in *fzo-1* mutants, mitochondrial fragmentation in Mt-GPAT mutants was rescued by knockdown of the pro-fission protein DRP-1. Third, in HeLa cells, fusion of mitochondria derived from two different cells after cell fusion was strongly inhibited by Mt-GPAT depletion. Mutation of LPAAT, which may increase the intracellular LPA level by blocking the conversion of LPA to PA, could rescue the mitochondrial fragmentation induced by *fzo-1* RNAi but not the mitochondrial fragmentation induced by *fzo-1* mutation. This result indicates that LPA cannot rescue the mitochondrial fragmentation unless FZO-1 is expressed. Alternatively, the *fzo-1* deletion may lead to an alternative compensatory response that is not influenced by LPA levels.

Mfn is degraded through the ubiquitin proteasome pathway that involves two E3 ligases, MITOL/March5 and Parkin (Cohen *et al*, 2008; Tanaka *et al*, 2010). The level of Mfn was not changed significantly in Mt-GPAT-depleted HeLa cells (Supplementary Figure S9E). In addition, the levels of Bax, Bak, Bcl-xL and Mfn-binding protein, MIB, which are known to modulate Mfn-mediated mitochondrial fusion (Eura *et al*, 2006; Karbowski *et al*, 2006; Rolland *et al*, 2009), were not changed in Mt-GPAT-depleted cells (Supplementary Figure S9E). Opa1 is involved in mitochondrial inner membrane fusion, and its function is controlled by proteolytic cleavage (Griparic *et al*, 2004; Ishihara *et al*, 2006). As previously reported (Griparic *et al*, 2007), Opa1 can be resolved into several bands on western blots in HeLa cells, and this band pattern was not altered by Mt-GPAT knockdown (Supplementary Figure S9E). Mfns form multimeric complexes that can be detected by blue native polyacrylamide gel electrophoresis (BN-PAGE). Oligomeric states of Mfns are changed in a GTP-dependent manner (Ishihara *et al*, 2004; Karbowski *et al*, 2006), and are modulated by Mfn regulators such as Bax and Bak (Karbowski *et al*, 2006). We detected endogenous Mfn oligomers from HeLa cells by BN-PAGE and found that their oligomeric states were GTP dependent (Supplementary Figure S11A). However, the oligomeric states were not changed by Mt-GPAT depletion or by addition of LPA *in vitro* (Supplementary Figure S11B and C). Mfn is a dynamin-like GTPase and its GTPase activity is required for

mitochondrial fusion (Santel and Fuller, 2001; Hoppins and Nunnari, 2009). We examined the effect of LPA on the GTPase activity of Mfn by using a recombinant rat Mfn produced by *E. coli* (Ishihara *et al*, 2004). Interestingly, addition of LPA to the reaction mixture slightly but significantly stimulated the Mfn1 GTPase activity (Supplementary Figure S11D–F). Lysophosphatidylcholine (LPC), which is inactive in rescuing the mitochondrial defect of Mt-GPAT mutants, did not stimulate GTPase activity (Supplementary Figure S11F). Although the stimulation was small in the detergent (Triton X-100)-containing *in vitro* assay, LPA produced on the mitochondrial outer membrane may stimulate GTPase activity of Mfn and enhance mitochondrial fusion.

Lipids also have roles in membrane dynamics (Chernomordik and Kozlov, 2008; Furt and Moreau, 2009). LPA is an inverted cone-shaped lipid that causes the membrane to have a positive curvature (Haucke and Di Paolo, 2007). In lipid bilayer fusion, hemifusion structures and fusion pores are characterized as sequences of the intermediate structures (Chernomordik and Kozlov, 2008). Lipids inducing positive curvature facilitate the formation of a fusion pore (Haucke and Di Paolo, 2007; Chernomordik and Kozlov, 2008). Therefore, LPA produced by Mt-GPAT may assist Mfn-mediated mitochondrial outer membrane fusion. Cardiolipin (CL) is predominantly localized in the mitochondrial inner membrane where it is synthesized from phosphatidylglycerol and cytidinediphosphate diacylglycerol. CL is required for optimal activities of many mitochondrial proteins (Hoffmann *et al*, 1994; Claypool *et al*, 2008). Loss of CL impacts on a variety of mitochondrial functions including mitochondrial fusion (Jiang *et al*, 2000; Choi *et al*, 2006; Gebert *et al*, 2009; Zhang *et al*, 2011). In Mt-GPAT mutants, the amount of CL was not affected (Supplementary Table S3), indicating that mitochondrial defect was not due to the decreased CL level in the mitochondria.

Mitochondrial phospholipase D (MitoPLD) has been identified as a key factor of mitochondrial fusion (Choi *et al*, 2006; Huang *et al*, 2011). MitoPLD hydrolyses CL on the outer mitochondrial membrane, resulting in the formation of PA. Overexpression of wild-type MitoPLD causes mitochondrial aggregation, whereas overexpression of catalytically inactive MitoPLD or RNAi-mediated knockdown of intrinsic MitoPLD causes mitochondrial fragmentation. Moreover, transient expression of Lipin 1b, one isoform of PA phosphatase, which may degrade MitoPLD-generated PA to diacylglycerol on the mitochondrial surfaces, induces the fission of long mitochondrial tubules into moderately sized fragments. Based on these results, the authors of the above studies postulated that PA facilitates mitochondrial fusion. A PA requirement has often been demonstrated in the SNARE-mediated fusion of secretary vesicles with the plasma membranes during many types of regulated exocytosis and during sporulation in yeast. Nonetheless, the mechanism through which MitoPLD-generated PA controls mitochondrial fusion remains unknown. LPA produced by Mt-GPAT could be acylated to form PA in the outer leaflet of the mitochondrial outer membranes. So far, LPAATs other than LPAAT1, LPAAT2/*acl-1*, *acl-2* in the ER have not been identified in either *C. elegans* or mammals. Moreover, our findings that the mitochondrial defect of Mt-GPAT mutants was rescued by metabolically stabilized LPA analogues and that the PA level was not decreased in *C. elegans* Mt-GPAT mutants or in Mt-GPAT-depleted HeLa cells (Supplementary Table S3) suggest that PA production through Mt-GPAT is not responsible for mitochondrial fusion. Thus, the MitoPLD/PA and Mt-GPAT/LPA pathways may work independently in mitochondrial fusion. PA is metabolically active; it can be dephosphorylated to form diacylglycerol, which was substantiated in MitoPLD-overexpressing cells (Huang *et al*, 2011), and it can be deacylated to form LPA. Another possibility is that MitoPLD-generated PA is further deacylated by an unknown enzyme to form LPA which functions in mitofusin-dependent mitochondrial fusion. The *C. elegans* genome does not have MitoPLD homologues, so that Mt-GPAT should dominate in supplying LPA for mitochondrial fusion.

Taken together, our results demonstrate that LPA produced by Mt-GPAT functions not only as a precursor for glycerolipid synthesis but also as an essential factor of mitochondrial fusion.

Materials and methods

Materials

[1-^{14}C]palmitic acid, [1-^{14}C]palmitoyl-CoA, and [1-^{14}C]oleoyl-CoA were purchased from American Radiolabeled Chemicals (St Louis, MO, USA). Glycerol-3-phosphate and 1-monopalmitoyl-rac-glycerol were purchased from Sigma. *sn*-1-palmitoyl lysophosphatidic acid, *sn*-1-palmitoyl-*sn*-2-oleoyl phosphatidic acid, *sn*-1-palmitoyl lysophosphatidylcholine, and *sn*-1-oleoyl lysophosphatidylserine were purchased from Avanti Polar Lipids (Alabaster, AL, USA). Stabilized LPA analogues, (2R)-1-oleoyl-2-*O*-methyl-glycerophosphothionate (OMPT), (3S)-1-fluoro-3-hydroxy-4-(linoleoyloxy) butyl-1-phosphonate (XY-26), and 1-palmitoyl alkyl LPA (XY-47), were synthesized and kindly provided by Dr Glenn D Prestwich at the University of Utah.

Acyltransferase assay

Synchronized young adult worms were suspended in 50 mM potassium phosphate buffer (pH 7.0) containing 0.15 M KCl, 1 mM EDTA, 1 mM dithiothreitol, 1 mM phenylmethanesulfonyl fluoride (PMSF) and 0.25 M sucrose (homogenizing buffer) and sonicated three times on ice for 30 s. The *C. elegans* homogenate was centrifuged at 1000 *g* for 5 min at 4°C. The resulting supernatant was further centrifuged at 105 000 *g* for 60 min. The pellet was suspended in homogenizing buffer (without EDTA, dithiothreitol, and PMSF) and used for the enzyme assay described below. HEK293 cells were harvested, washed with ice-cold phosphate-buffered saline, and sonicated three times on ice for 5 s in homogenizing buffer. The membrane fraction of HEK293 cells was prepared as described above. GPAT activity was assayed at 20°C for 30 min (*C. elegans*) or 37°C for 15 min (HEK293 cells) in a 200-μl reaction mixture containing 75 mM Tris/HCl, pH 7.5, 4 mM $MgCl_2$, 1 mg/ml bovine serum albumin free fatty acids, 8 mM NaF, 800 μM glycerol-3-phosphate, 40 μM [^{14}C]palmitoyl-CoA, and 45 μg (*C. elegans*) or 10 μg (HEK293 cells) protein of the membrane fraction. LPAAT activity was measured at 20°C for 5 min in a 800 μl reaction mixture containing 100 mM Tris/HCl, pH 7.5, 1 mg/ml bovine serum albumin free fatty acids, 40 μM 1-oleoyl lysophosphatidic acid, 20 μM LPA analogue, 12.5 μM [^{14}C]oleoyl-CoA, and 5 μg protein of the membrane fraction. The acyltransferase reaction was stopped by mixing with methanol. The lipids were extracted by the method of Bligh and Dyer (1959) and separated by TLC in chloroform/methanol/water (65/25/4, v/v) and the amount of radioactivity was analysed with a bioimaging analyzer (BAS-1500, FUJIFILM).

Lipid analysis

Content of phospholipids and triacylglycerol. Lipids of synchronized young adult worms were extracted by the method of Bligh and Dyer. The phosphorus contents of the total lipids were determined by the method of Bartlett (1959). The triacylglycerol

contents were measured using enzymatic kit (Wako Triglyceride E-test, Wako Pure Chemical Ltd., Osaka, Japan).

In vivo incorporation of exogenous fatty acids into C. elegans. Incorporation of exogenous fatty acids into *C. elegans* was analysed as described previously (Lee *et al*, 2008). Synchronized first-stage larvae (800–1200 animals) were cultured with 1 μCi of [^{14}C]palmitic acid on NGM plates at 20°C until they reached the young adult stage. Lipids of young adult worms were extracted by the method of Bligh and Dyer and separated by one-dimensional TLC on silica gel 60 plates (Merck) in chloroform/ethanol/water/triethylamine (30/35/7/35, v/v). Then, the area of silica gel corresponding to neutral lipids was scraped off the plates, and the lipids was re-extracted and separated by TLC in petroleum ether/ethyl ether/acetic acid (60/40/1, v/v). Incorporation of [^{14}C]palmitic acid into triacylglycerol was expressed as the percentage of radioactivity incorporated into total lipids.

Contents of CL and phosphatidic acid. Lipids of young adult worms and HeLa cells were extracted by the method of Bligh and Dyer and separated by one-dimensional TLC on silica gel 60 plates (Merck) in chloroform/methanol/water/ammonium hydroxide (60:37.5:3:1, v/v). Then, the area of silica gel corresponding to CL or phosphatidic acid was scraped off the plates, and the lipids were re-extracted and the phosphorus contents of each lipid were determined as described above.

MitoTracker staining

C. elegans. Young adult worms were transferred to NGM plates containing 2 μM MitoTracker Red CMXRos (Molecular Probes, Inc., Eugene, OR) and incubated for 2 days in the dark. Worms were washed with M9 buffer, mounted on an agar pad and images were taken by using a confocal fluorescence microscope (LSM510; Carl Zeiss Inc., Thornwood, NY, USA).

HeLa cells. HeLa cells were incubated with 500 nM MitoTracker Red CM-H_2XMRos (Molecular Probes, Inc.) for 40 min before fixation and imaged as described above.

Electron microscopy

Synchronized 72-h-old adult worms or HeLa cells were pre-fixed with 4% paraformaldehyde and 1% glutaraldehyde in 0.1 M phosphate buffer (pH 7.4). Samples were then cut into small pieces, fixed again with 2% paraformaldehyde and 2% glutaraldehyde in the same buffer, and post-fixed with 2% osmium tetroxide in phosphate buffer for 4 h. Fixed specimens were dehydrated in a graded series of ethanol and embedded in Quetol 651 epoxy resin. Ultrathin (80 to 90 nm-thick) sections obtained by ultramicrotomy were stained with uranyl acetate for 15 min and with modified Sato's lead solution for 5 min. TEM observation was performed using a JEOL JEM-1200EX electron microscope. For the quantification of mitochondrial length in HeLa cells, over 350 mitochondria were measured per siRNA condition using ImageJ (NIH, USA).

Injection of lipids into C. elegans germ cells

Each lipid was diluted in TE buffer to 50 μM and was microinjected into the gonads of *acl-6* mutants at the L4 stage. After injection, worms were transferred to NGM plates containing 2 μM MitoTracker Red CMXRos (Molecular Probes, Inc.) and incubated for 2 days in the dark.

Mitochondrial fusion assay

Mitochondrial fusion assay was performed as described previously (Cipolat *et al*, 2004), except that HeLa cells stably expressing su9-GFP and su9-RFP (Taguchi *et al*, 2007) were used.

Supplementary data

Supplementary data are available at *The EMBO Journal* Online (http://www.embojournal.org).

Acknowledgements

We thank T Taguchi (University of Tokyo) for helpful discussions; H Fukuda for technical support; A Fire (Stanford University School of Medicine) for plasmids; and the *Caenorhabditis* Genetics Center (University of Minnesota, Minneapolis) for strains. This work was supported by the Core Research for Evolutional Science and Technology, Japan Science and Technology Agency (HA), the Program for Promotion of Basic and Applied Research for Innovations in Bio-Oriented Industry (HA), Grants-in-aid from the Japanese Ministry of Education, Culture, Sports, Science, and Technology and the Japanese Ministry of Health, Labor, and Welfare (to HA).

Author contributions: YO, TS, EKN, NHT, and NK carried out the experiments. All authors discussed the results and designed the experimental approaches. TI and HA wrote the manuscript.

Conflict of interest

The authors declare that they have no conflict of interest.

References

Aoki J, Inoue A, Okudaira S (2008) Two pathways for lysophosphatidic acid production. *Biochim Biophys Acta* **1781:** 513–518

Artal-Sanz M, Tsang WY, Willems EM, Grivell LA, Lemire BD, van der Spek H, Nijtmans LG, Sanz MA (2003) The mitochondrial prohibitin complex is essential for embryonic viability and germline function in *Caenorhabditis elegans*. *J Biol Chem* **278:** 32091–32099

Bartlett GR (1959) Phosphorous assay in column chromatography. *J Biol Chem* **234:** 466–468

Beigneux AP, Vergnes L, Qiao X, Quatela S, Davis R, Watkins SM, Coleman RA, Walzem RL, Philips M, Reue K, Young SG (2006) Agpat6—a novel lipid biosynthetic gene required for triacylglycerol production in mammary epithelium. *J Lipid Res* **47:** 734–744

Bligh EG, Dyer WJ (1959) A rapid method of total lipid extraction and purification. *Can J Biochem Physiol* **37:** 911–917

Bratic I, Hench J, Henriksson J, Antebi A, Burglin TR, Trifunovic A (2009) Mitochondrial DNA level, but not active replicase, is essential for *Caenorhabditis elegans* development. *Nucleic Acids Res* **37:** 1817–1828

Chen H, Detmer SA, Ewald AJ, Griffin EE, Fraser SE, Chan DC (2003) Mitofusins Mfn1 and Mfn2 coordinately regulate mitochondrial fusion and are essential for embryonic development. *J Cell Biol* **160:** 189–200

Chen YQ, Kuo MS, Li S, Bui HH, Peake DA, Sanders PE, Thibodeaux SJ, Chu S, Qian YW, Zhao Y, Bredt DS, Moller DE, Konrad RJ, Beigneux AP, Young SG, Cao G (2008) AGPAT6 is a novel microsomal glycerol-3-phosphate acyltransferase. *J Biol Chem* **283:** 10048–10057

Chernomordik LV, Kozlov MM (2008) Mechanics of membrane fusion. *Nat Struct Mol Biol* **15:** 675–683

Choi SY, Huang P, Jenkins GM, Chan DC, Schiller J, Frohman MA (2006) A common lipid links Mfn-mediated mitochondrial fusion and SNARE-regulated exocytosis. *Nat Cell Biol* **8:** 1255–1262

Cipolat S, de Brito OM, Dal Zilio B, Scorrano L (2004) OPA1 requires mitofusin 1 to promote mitochondrial fusion. *Proc Natl Acad Sci USA* **101:** 15927–15932

Claypool SM, Oktay Y, Boontheung P, Loo JA, Koehler CM (2008) Cardiolipin defines the interactome of the major ADP/ATP carrier protein of the mitochondrial inner membrane. *J Cell Biol* **182:** 937–950

Cohen MM, Leboucher GP, Livnat-Levanon N, Glickman MH, Weissman AM (2008) Ubiquitin-proteasome-dependent degradation of a mitofusin, a critical regulator of mitochondrial fusion. *Mol Biol Cell* **19:** 2457–2464

Coleman RA, Lee DP (2004) Enzymes of triacylglycerol synthesis and their regulation. *Prog Lipid Res* **43:** 134–176

Coleman RA, Lewin TM, Muoio DM (2000) Physiological and nutritional regulation of enzymes of triacylglycerol synthesis. *Annu Rev Nutr* **20:** 77–103

Detmer SA, Chan DC (2007) Functions and dysfunctions of mitochondrial dynamics. *Nat Rev Mol Cell Biol* **8:** 870–879

Dircks LK, Ke J, Sul HS (1999) A conserved seven amino acid stretch important for murine mitochondrial glycerol-3-phosphate acyltransferase activity: significance of arginine 318 in catalysis. *J Biol Chem* **274:** 34728–34734

Dowhan W (1997) Molecular basis for membrane phospholipid diversity: why are there so many lipids? *Annu Rev Biochem* **66:** 199–232

Eura Y, Ishihara N, Oka T, Mihara K (2006) Identification of a novel protein that regulates mitochondrial fusion by modulating mitofusin (Mfn) protein function. *J Cell Sci* **119:** 4913–4925

Eura Y, Ishihara N, Yokota S, Mihara K (2003) Two mitofusin proteins, mammalian homologues of FZO, with distinct functions are both required for mitochondrial fusion. *J Biochem* **134:** 333–344

Furt F, Moreau P (2009) Importance of lipid metabolism for intracellular and mitochondrial membrane fusion/fission processes. *Int J Biochem Cell Biol* **41:** 1828–1836

Gebert N, Joshi AS, Kutik S, Becker T, McKenzie M, Guan XL, Mooga VP, Stroud DA, Kulkarni G, Wenk MR, Rehling P, Meisinger C, Ryan MT, Wiedemann N, Greenberg ML, Pfanner N (2009) Mitochondrial cardiolipin involved in outer-membrane protein biogenesis: implications for Barth syndrome. *Curr Biol* **19:** 2133–2139

Gimeno RE, Cao J (2008) Mammalian glycerol-3-phosphate acyltransferases: newgenes for an old activity. *J Lipid Res* **49:** 2079–2088

Griparic L, Kanazawa T, van der Bliek AM (2007) Regulation of the mitochondrial dynamin-like protein Opa1 by proteolytic cleavage. *J Cell Biol* **178:** 757–764

Griparic L, van der Wel NN, Orozco IJ, Peters PJ, van der Bliek AM (2004) Loss of the intermembrane space protein Mgm1/OPA1 induces swelling and localized constrictions along the lengths of mitochondria. *J Biol Chem* **279:** 18792–18798

Hammond LE, Albright CD, He L, Rusyn I, Watkins SM, Doughman SD, Lemasters JJ, Coleman RA (2007) Increased oxidative stress is associated with balanced increases in hepatocyte apoptosis and proliferation in glycerol-3-phosphate acyltransferase-1 deficient mice. *Exp Mol Pathol* **82:** 210–219

Hammond LE, Gallagher PA, Wang S, Hiller S, Kluckman KD, Posey-Marcos EL, Maeda N, Coleman RA (2002) Mitochondrial glycerol-3-phosphate acyltransferase-deficient mice have reduced weight and liver triacylglycerol content and altered glycerolipid fatty acid composition. *Mol Cell Biol* **22:** 8204–8214

Hammond LE, Neschen S, Romanelli AJ, Cline GW, Ilkayeva OR, Shulman GI, Muoio DM, Coleman RA (2005) Mitochondrial glycerol-3-phosphate acyltransferase-1 is essential in liver for the metabolism of excess acyl-CoAs. *J Biol Chem* **280:** 25629–25636

Haucke V, Di Paolo G (2007) Lipids and lipid modifications in the regulation of membrane traffic. *Curr Opin Cell Biol* **19:** 426–435

Hoffmann B, Stockl A, Schlame M, Beyer K, Klingenberg M (1994) The reconstituted ADP/ATP carrier activity has an absolute requirement for cardiolipin as shown in cysteine mutants. *J Biol Chem* **269:** 1940–1944

Hoppins S, Nunnari J (2009) The molecular mechanism of mitochondrial fusion. *Biochim Biophys Acta* **1793:** 20–22

Huang H, Gao Q, Peng X, Choi SY, Sarma K, Ren H, Morris AJ, Frohman MA (2011) piRNA-associated germline nuage formation and spermatogenesis require MitoPLD pro-fusogenic mitochondrial-surface lipid signaling. *Dev Cell* **20:** 376–387

Hubbard EJA, Greenstein D (2005) Introduction to the germ line. In *Worm book*, The *C. elegans* Research Community (ed) WormBook, doi/10.1895/wormbook.1.18.1, http://www.wormbook.org

Ichishita R, Tanaka K, Sugiura Y, Sayano T, Mihara K, Oka T (2008) An RNAi screen for mitochondrial proteins required to maintain the morphology of the organelle in *Caenorhabditis elegans*. *J Biochem* **143:** 449–454

Imae R, Inoue T, Kimura M, Kanamori T, H.Tomioka N, Kage-Nakadai E, Mitani S, Arai H (2010) Intracellular phospholipase A1 and acyltransferase, which are involved in *Caenorhabditis elegans* stem cell divisions, determine the *sn*-1 fatty acyl chain of phosphatidylinositol. *Mol Biol Cell* **21:** 3114–3124

Ishihara N, Eura Y, Mihara K (2004) Mitofusin 1 and 2 play distinct roles in mitochondrial fusion reactions via GTPase activity. *J Cell Sci* **117:** 6535–6546

Ishihara N, Fujita Y, Oka T, Mihara K (2006) Regulation of mitochondrial morphology through proteolytic cleavage of OPA1. *EMBO J* **25:** 2966–2977

Jiang F, Ryan MT, Schlame M, Zhao M, Gu Z, Klingenberg M, Pfanner N, Greenberg ML (2000) Absence of cardiolipin in the crd1 null mutant results in decreased mitochondrial membrane potential and reduced mitochondrial function. *J Biol Chem* **275:** 22387–22394

Karbowski M, Norris KL, Cleland MM, Jeong SY, Youle RJ (2006) Role of Bax and Bak in mitochondrial morphogenesis. *Nature* **443:** 658–662

Kent C (1995) Eukaryotic phospholipid biosynthesis. *Annu Rev Biochem* **64:** 315–343

Kimble J, Crittenden SL (2005) Germline proliferation and its control. In *Worm book*, The *C. elegans* Research Community (ed) WormBook, doi/10.1895/wormbook.1.13.1, http://www.wormbook.org

Labrousse AM, Zappaterra MD, Rube DA, van der Bliek AM (1999) *C. elegans* dynamin-related protein DRP-1 controls severing of the mitochondrial outer membrane. *Mol Cell* **4:** 815–826

Lee HC, Inoue T, Imae R, Kono N, Shirae S, Matsuda S, Gengyo-Ando K, Mitani S, Arai H (2008) *Caenorhabditis elegans* mboa-7, a member of the MBOAT family, is required for selective incorporation of polyunsaturated fatty acids into phosphatidylinositol. *Mol Biol Cell* **19:** 1174–1184

Lewin TM, Schwerbrock NM, Lee DP, Coleman RA (2004) Identification of a new glycerol-3-phosphate acyltransferase isoenzyme, mtGPAT2, in mitochondria. *J Biol Chem* **279:** 13488–13495

Nagle CA, Vergnes L, Dejong H, Wang S, Lewin TM, Reue K, Coleman RA (2008) Identification of a novel *sn*-glycerol-3-phosphate acyltransferase isoform, GPAT4, as the enzyme deficient in *Agpat6*$^{-/-}$ mice. *J Lipid Res* **49:** 823–831

Neschen S, Morino K, Hammond LE, Zhang D, Liu ZX, Romanelli AJ, Cline GW, Pongratz RL, Zhang WM, Choi CS, Coleman RA, Shulman GI (2005) Prevention of hepatic steatosis and hepatic insulin resistance in mitochondrial acyl-CoA: glycerol-sn-3-phosphate acyltransferase 1 knockout mice. *Cell Metab* **2:** 55–65

Neuwald AF (1997) Barth syndrome may be due to an acyltransferase deficiency. *Curr Biol* **7:** R465–R466

Okamoto K, Shaw JM (2005) Mitochondrial morphology and dynamics in yeast and multicellular eukaryotes. *Annu Rev Genet* **39:** 503–536

Pitt JN, Schisa JA, Priess JR (2000) P granules in the germ cells of *Caenorhabditis elegans* adults are associated with clusters of nuclear pores and contain RNA. *Dev Biol* **219:** 315–333

Rojo M, Legros F, Chateau D, Lombès A (2002) Membrane topology and mitochondrial targeting of mitofusins, ubiquitous mammalian homologs of the transmembrane GTPase Fzo. *J Cell Sci* **115:** 1663–1674

Rolland SG, Lu Y, David CN, Conradt B (2009) The BCL-2-like protein CED-9 of C. elegans promotes FZO-1/Mfn1,2- and EAT-3/Opa1- dependent mitochondrial fusion. *J Cell Biol* **186:** 525–540

Santel A, Frank S, Gaume B, Herrler M, Youle R, Fuller MT (2003) Mitofusin-1 protein is a generally expressed mediator of mitochondrial fusion in mammalian cells. *J Cell Sci* **116:** 2763–2774

Santel A, Fuller MT (2001) Control of mitochondrial morphology by a human mitofusin. *J Cell Sci* **114:** 867–874

Sesaki H, Jensen RE (1999) Division versus fusion: Dnm1p and Fzo1p antagonistically regulate mitochondrial shape. *J Cell Biol* **147:** 699–706

Sijen T, Fleenor J, Simmer F, Thijssen KL, Parrish S, Timmons L, Plasterk RHA, Fire A (2001) On the role of RNA amplification in dsRNA-triggered gene silencing. *Cell* **107:** 465–476

Smirnova E, Griparic L, Shurland DL, van der Bliek AM (2001) Dynamin-related protein Drp1 is required for mitochondrial division in mammalian cells. *Mol Biol Cell* **12:** 2245–2256

Smirnova E, Shurland DL, Ryazantsev SN, van der Bliek AM (1998) A human dynamin-related protein controls the distribution of mitochondria. *J Cell Biol* **143:** 351–358

Taguchi N, Ishihara N, Jofuku A, Oka T, Mihara K (2007) Mitotic phosphorylation of dynamin-related GTPase Drp1 participates in mitochondrial fission. *J Biol Chem* **282:** 11521–11529

Takeuchi K, Reue K (2009) Biochemistry, physiology, and genetics of GPAT, AGPAT, and lipin enzymes in triglyceride synthesis. *Am J Physiol Endocrinol Metab* **296:** E1195–E1209

Tanaka A, Cleland MM, Xu S, Narendra DP, Suen DF, Karbowski M, Youle RJ (2010) Proteasome and p97 mediate mitophagy and degradation of mitofusins induced by Parkin. *J Cell Biol* **191:** 1367–1380

van Meeteren LA, Moolenaar WH (2007) Regulation and biological activities of the autotaxin-LPA axis. *Prog Lipid Res* **46:** 145–160

Vergnes L, Beigneux AP, Davis R, Watkins SM, Young SG, Reue K (2006) *Agpat6* deficiency causes subdermal lipodystrophy and resistance to obesity. *J Lipid Res* **47:** 745–754

Wendel AA, Lewin TM, Coleman RA (2009) Glycerol-3-phosphate acyltransferases: rate limiting enzymes of triacylglycerol biosynthesis. *Biochim Biophys Acta* **1791:** 501–506

Westermann B (2008) Molecular machinery of mitochondrial fusion and fission. *J Biol Chem* **283:** 13501–13505

Xu Y, Aoki J, Shimizu K, Umezu-Goto M, Hama K, Takanezawa T, Yu S, Mills GB, Arai H, Qian L, Prestwich GD (2005) Structure-activity relationships of fluorinated lysophosphatidic acid analogues. *J Med Chem* **48:** 3319–3327

Yazdi M, Ahnmark A, William-Olsson L, Snaith M, Turner N, Osla F, Wedin M, Asztely AK, Elmgren A, Bohlooly YM, Schreyer S, Linden D (2008) The role of mitochondrial glycerol-3-phosphate acyltransferase-1 in regulating lipid and glucose homeostasis in highfat diet fed mice. *Biochem Biophys Res Commun* **369:** 1065–1070

Ye X, Chun J (2010) Lysophosphatidic acid (LPA) signaling in vertebrate reproduction. *Trends Endocrinol Metab* **21:** 17–24

Zhang J, Guan Z, Murphy AN, Wiley SE, Perkins GA, Worby CA, Engel JL, Heacock P, Nguyen OK, Wang JH, Raetz CRH, Dowhan W, Dixon JE (2011) Mitochondrial phosphatase PTPMT1 is essential for cardiolipin biosynthesis. *Cell Metab* **13:** 690–700